Rational disruption of the oligomerization of the mini-ferritin *E. coli* DPS through protein-protein interface mutation

Yu Zhang, Jing Fu, Sze Y. Chee, Emmiline X. W. Ang, and Brendan P. Orner*

Division of Chemistry and Biological Chemistry, School of Physical & Mathematical Sciences, Nanyang Technological University, Singapore 637371

Received 27 June 2011; Revised 24 August 2011; Accepted 26 August 2011
DOI: 10.1002/pro.731
Published online 6 September 2011 proteinscience.org

Abstract: DNA-binding protein from starved cells (DPS), a mini-ferritin capable of self-assembling into a 12-meric nano-cage, was chosen as the basis for an alanine-shaving mutagenesis study to investigate the importance of key amino acid residues, located at symmetry-related protein-protein interfaces, in controlling protein stability and self-assembly. Nine mutants were designed through simple inspection, synthesized, and subjected to transmission electron microscopy, circular dichroism, size exclusion chromatography, and "virtual alanine scanning" computational analysis. The data indicate that many of these residues may be hot spot residues. Most remarkably, two residues, R83 and R133, were observed to shift the oligomerization state to ~50% dimer. Based on the hypothesis that these two residues constitute a "hot strip," located at the ferritin-like threefold axis, the double mutant was generated which completely shuts down detectable formation of 12-mer in solution, favoring a cooperatively folded dimer. The fact that this effect logically builds upon the single mutants emphasizes that complex self-assembly has the potential to be manipulated rationally. This study should have an impact on the fundamental understanding of the assembly of DPS protein cages specifically and protein quaternary structure in general. In addition, as there is much interest in applying these and similar systems to the templation of nano-materials and drug delivery, the ability to control this ferritin's oligomerization state and stability could prove especially valuable.

Keywords: nano-cage; ferritin; DPS; alanine shaving; self-assembly

Introduction

Protein-protein interactions play key roles in signal transduction and are essential for many disease-related and, therefore, medicinally-relevant processes.[1,2] Moreover, protein-protein interactions are also integral to the generation of cellular self-assembled nano-structures, and establishing how they control self-assembly could lead not only to fundamental understanding but also to the eventual rational design of novel structures for a myriad of applications such as the templation of inorganic nano-materials and for encapsulated reaction chemistry.[3–8]

Although protein-protein interactions are intriguing medicinal targets, they have only recently been pursued for drug development studies somewhat owing to the discovery that although they often involve large, buried surface area, they can be inhibited using low molecular weight small molecules that target "hot spot" residues where the binding energy is concentrated.[9,10] Alanine shaving,

Abbreviations: BFR, Bacterioferritin; DPS, DNA binding protein from starved cells; Ek, enterokinase; LIC, ligation-independent cloning; SEC, size exclusion chromatography; TEM, transmission electron microscopy.

Additional Supporting Information may be found in the online version of this article.

Conflict of interest: This research was partially supported through B. P. O.'s personal salary.

Grant sponsor: CBC start up grant and a Singapore Ministry of Education Academic Research Fund Tier 1 Grant; Grant number: RG 53/06.

**Correspondence to:* Brendan P. Orner, Division of Chemistry and Biological Chemistry, School of Physical & Mathematical Sciences, Nanyang Technological University, Singapore 637371. E-mail: orner@ntu.edu.sg

where individual side changes are conceptually shaved to a methyl residuum and where the stabilities of the resulting mutants are determined with respect to wild type, is the most common method to identify hot spot residues.[11–13] This study uses alanine shaving to identify hot spots in a mini-ferritin nano-cage protein.

Ferritins are iron storage proteins that self-assemble into spherical, hollow nano-cages through protein-protein interactions between four-helix bundle monomers.[14–17] The homo-oligomerization and tractable self-assembly mechanism of ferritins make them an ideal system to understand the vital role protein-protein interactions play in protein folding and in higher order quaternary structure.

DNA-binding protein from starved cells (DPS) proteins and bacterioferritin (BFR) both belong to the ferritin superfamily of proteins and are considered mini- and maxi-ferritins because they are made up of 12 and 24 monomers, respectively.[14] We have recently performed alanine shaving of the protein-protein interfaces in the maxi-ferritin BFR from *Escherichia coli* to identify residues that control its stability and oligomerization.[18,19]

As an extension of this latter work, we describe here the application of this strategy to *E. coli* DPS (*Ec*DPS). Because the structural energetics of the two proteins are quite unique, this is a distinct application of the strategy. DPS proteins are mini-ferritins composed of identical monomers that assemble into a hollow, tetrahedrally symmetric sphere, whereas the maxi-ferritins form hollow oligomeric spheres with octahedral symmetry.[14] *Ec*DPS assembles into a cage with two and threefold symmetry axes and interior and exterior diameters of 45 Å and 90 Å, respectively (Figs. 1 and 2) whereas the *Ec*BFR cage additionally has fourfold symmetry axes and is 75 Å and 120 Å in interior and exterior diameter, respectively. We and others have demonstrated that this maxi-ferritin exists as a mixture between the 24-mer cage and the dimer whereas *Ec*DPS assembles solely into a 12-mer.

The *Ec*DPS monomer has a four-helix bundle fold that shares structural homology with the *Ec*BFR monomer. In both structures, the first two helices (the A and B helices) are connected by a short loop, as are the last two helices (the C and D helices). A long linker that stretches across the surface of the four-helix bundle connects the two pairs of helices. In *Ec*BFR, there is no secondary structure in the BC linker, however, for *Ec*DPS it folds into a short extra-bundle helix, and this BC helix interacts with another across the twofold symmetric, dimeric interface. *Ec*BFR has a unique C-terminal E helix that helps to establish the fourfold symmetry axes with four monomers. In addition, the termini of the A and D helices of *Ec*BFR are a bit longer than those of *Ec*DPS (Fig. 1). We have previously investigated the role that the small, extra-bundle helices (E helix in BFR and BC helix in DPS) play in the stability and oligomerization of both *Ec*DPS and *Ec*BFR. Emphasizing the distinctions between the two proteins, we found that the E helix in BFR plays a strong role in the formation of quaternary structure whereas the BC helix of DPS has only a very small role if any.[18]

Moreover, how the quaternary structure relates to the enzymology of the two proteins further stresses their distinctness. In the Dps family, the ferrioxidase center is located at the twofold symmetry axis between two monomers rather than being embedded in the four-helix bundle of a single subunit in BFR.[14,20]

So, although the monomer structures are similar, clearly, the underlying fundamentals that control the oligomer architecture and how these relate to the activity of these two subfamilies of protein cages are significantly different. Establishing the similarities and divergences in these proteins' structural energetics is an initial step in our long-term goal of converting, with a minimum of mutations, a mini-ferritin monomer into one that assembles into a maxi-ferritin and vice versa. Therefore, it is of great value to further scrutinize the rudiments of these related structures by investigating the role key protein-protein interactions play in the assembly and stability of the DPS mini-ferritin.

Results

Selection of interfacial residues for mutagenesis

We targeted interfacial residues involved in salt bridges, because their identification is relatively straightforward from inspection of the crystal structure, and those that are aromatic due to the fact that they have a high tendency to be part of energetic hot spots.[12,13] The protein has three types of protein-protein interfaces that are related to the twofold and the Dps-like and the ferritin-like threefold symmetry axes. The Dps-like threefold interface buries only a small amount of monomer surface area, and salt bridging interactions or aromatic amino acids that are prevalent in hot spots (Trp or Tyr) are not evident in this interface. Computational analysis (see below) confirms that it may not be the most fertile interface for our hot spot search (Supporting Information Fig. S12). Therefore, the selection of potential hot spot residues was mainly focused on the twofold and the ferritin-like threefold interfaces. Through simple inspection of the *E. coli* DPS crystal structure (PDB ID: 1dps) eight such residues were identified.[14] Thus, Y16, R18, W52, D78, R83, R133, D146, and W160 were selected for mutagenesis (Fig. 2).

Two of these, W52 and D78, make twofold symmetric contacts near the ferroxidase center.[14,18,21] It

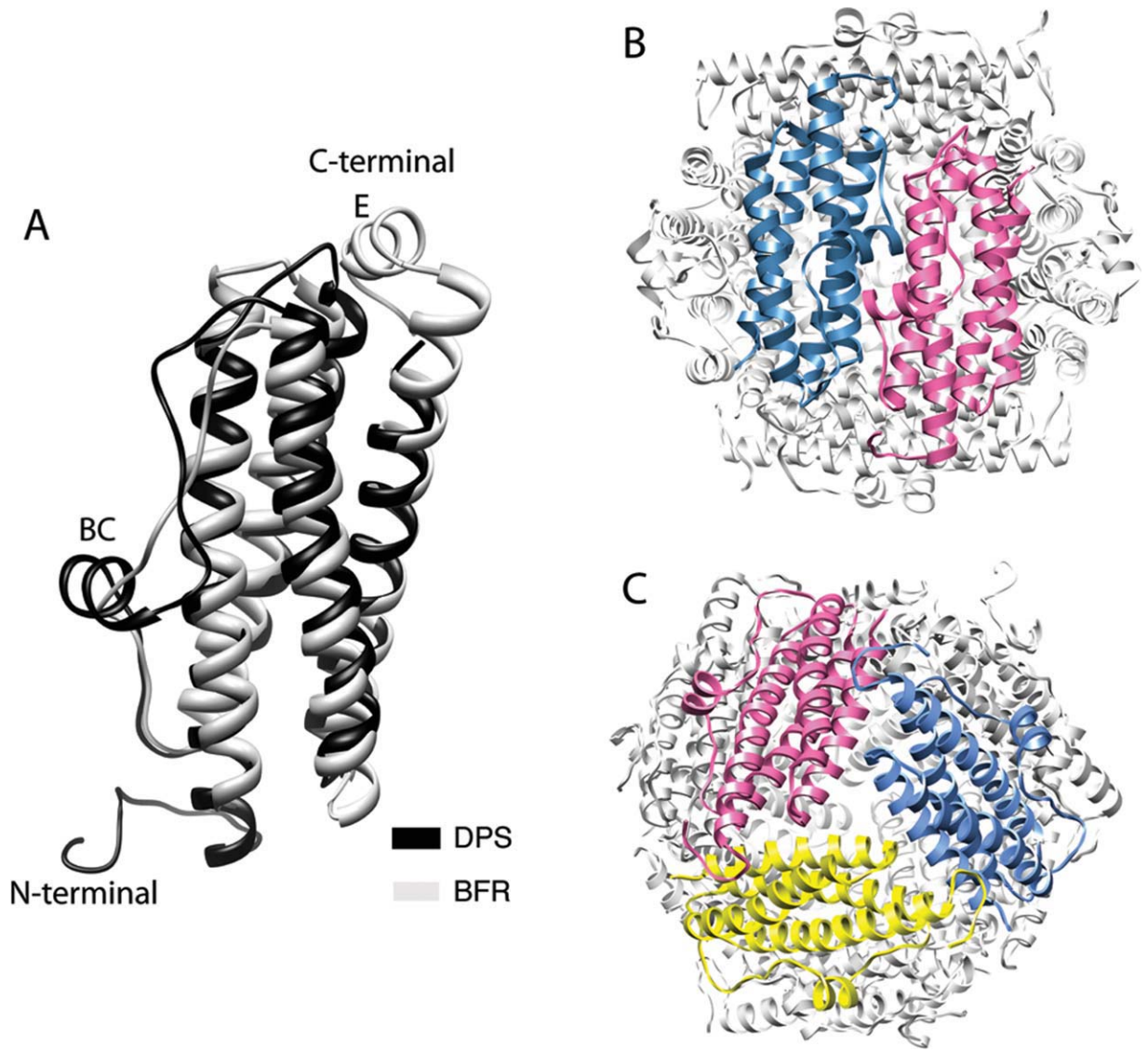

Figure 1. (A) Superimposition of BFR (grey) and DPS (dark) monomers generated using the DaliLite online program (http://www.ebi.ac.uk/Tools/dalilite/index.html). DPS protein cages viewed along a (B) twofold axis and (C) ferritin-like threefold axis. (PDB ID: 1dps and 1bfr).

should be noted that the aromatic residue W52 was identified at both the twofold and the Dps-like threefold interface by Protein Interfaces, Surfaces and Assemblies (PISA)[22] analysis, however, the energetic effect was predicted to be more significant at the twofold interface (data not shown). The acidic residue D78 appears to be interacting with both K48 and R70 [Fig. 4(A)].

Five of the selected residues, R18, R83, R133, D146, and W160, are positioned around the ferritin-like threefold symmetry axes. Intriguingly, the acidic residue, D146, is located near an ion channel which has been shown to have a negative electrostatic gradient which guides iron toward the ferroxidase centers.[21] Residue R18 appears to form salt bridges with E163 and D123 [Fig. 4(B)]. Residues R83 and R133 seem to be part of an extended network involving D143, D156, and D20 [Fig. 4(B)]. For these two residues, we reasoned that whatever effect the single mutations might have would be amplified in concert. Therefore, the double mutant R83A/R133A was also chosen for study.[23] The aromatic residue, W160, is located at both types of threefold interfaces, but, again, the energetic effect at the ferritin-like threefold interface is predicted to be more significant than at the Dps-like symmetry interface (Supporting Information Figs. S11 and S12).

Sequence alignment of DPS proteins from 13 diverse species revealed that six of the residues selected for mutation are conserved (Fig. 3). The remaining two, Y16 and R18, are located in an extended N-terminal region that is not present in the majority of the proteins analyzed. However, other proteins with this domain, such as DPS from *Yersinia pestis*, have Tyr and Arg residues in identical positions.

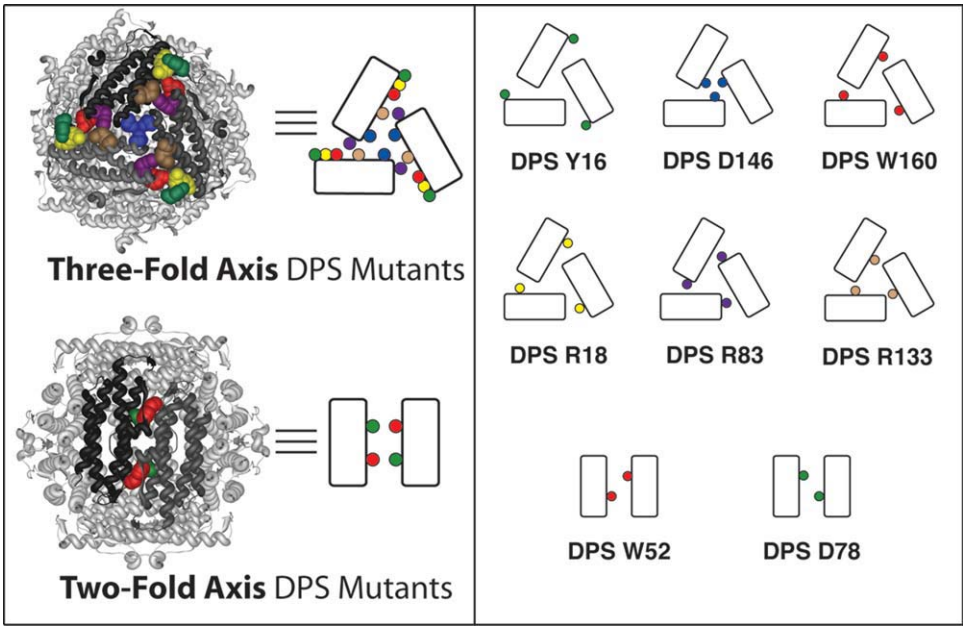

Figure 2. Predicted structurally and energetically important residues at the protein-protein interfaces of the nano-cage protein, *E. coli* DPS. (Left) The DPS crystal structure (PDB ID: 1dps) with mutated residues highlighted with respect to the axes of symmetry and schematized diagrams representing the protein-protein interactions defining these symmetries. (Right) The residues of DPS mutated in this study and their schematized position at the symmetry related protein-protein interfaces. This schematic convention is conserved throughout the article.

After selection by structural inspection, virtual alanine scanning was performed to support the prediction that these would be energetically important residues (Supporting Information Figs. S10–S12).[24] A calculated $\Delta\Delta G$ of greater than 1 kcal/mol in this analysis suggests that a residue may be an energetic hot spot, and all but one of our selected residues were predicted to be hot spots. The outlier was Y16. Because it is somewhat solvent exposed, the calculation did not identify it as an interfacial residue. However, analysis using PISA identifies it as a residue both at the twofold and ferritin-like threefold interfaces though the buried surface area is low (data not shown). Therefore, we decided to generate this mutant. Additionally, the residue D146 was predicted to be only a weak hot spot. Because of the placement of this residue at an important ion channel (see above) this mutant was also produced. Of the selected residues R83 and R133 were predicted to be the energetically most significant. These nine mutants were successfully cloned, expressed, and purified (Supporting Information Figs. S1–S4).

TEM analysis of protein assembly

To determine whether the selected residues affect the ability of DPS to assemble into nano-cages, the mutants were imaged with TEM. The resulting electron micrographs indicated that all the proteins, except the double mutant DPS R83A/R133A, formed nano-cages under these conditions. Image analysis demonstrated that the size of DPS is similar to that measured by Grant *et al*.[14] The size of the mutants from image analysis (ImageJ) was either equal to or slightly larger than the wild-type protein (Fig. 5 and Supporting Information Fig. S7) with DPS Y16A being significantly larger than DPS which may be because of loose packing in the mutant. These results suggest that single point mutation does not alter the energetics to an extent that would disrupt self-assembly although double mutation does. It should be mentioned that in similar systems we have observed that conditions for obtaining TEM micrographs can encourage oligomerization that is not observed in solution.[19]

Size exclusion chromatographic determination of assembly in solution

To determine the role the mutated residues play in assembly in solution, the mutants were analyzed by size exclusion chromatography (SEC) (Fig. 6 and Supporting Information Fig. S13). The retention volumes of each species were correlated to the molecular weights of protein standards (Supporting Information Figs. S5 and S6), which were then used to calculate approximate oligomerization states. Wild-type DPS protein formed solely 12-mer, consistent with the literature.[18,25,26] All the DPS single mutants assembled into 12-mers but four mutants also formed smaller oligomers. Mutation of W52 resulted in some unassembled monomer (6%) and

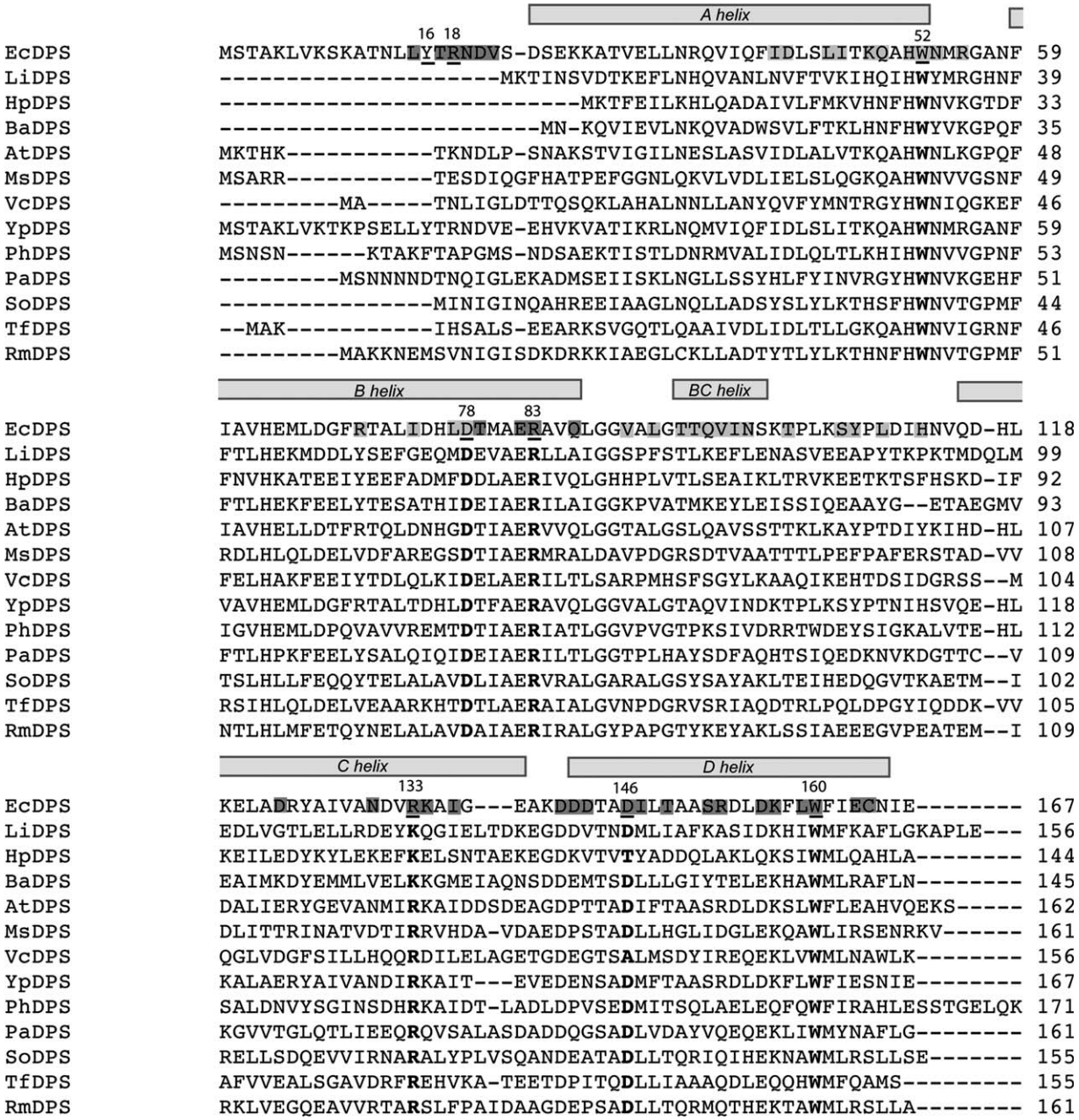

Figure 3. Sequence alignment of representative DPS proteins. EcDPS, *E. coli* Dps homolog; LiDPS, *Listeria innocua* Dps homolog; HpDPS, *Helicobacter pylori* Dps homolog; BaDPS, *Bacillus anthracis* Dps homolog; AtDPS, *Agrobacterium tumefaciens* Dps homolog; MsDPS, *Mycobacterium smegmatis* Dps homolog; VcDPS, *Vibrio cholerae* Dps homolog; YpDPS, *Yersinia pestis* Dps homolog; PhDPS, *Pseudoalteromonas haloplanktis* Dps homolog; PaDPS, *Psychrobacter arcticus* Dps homolog; SoDPS, *Shewanella oneidensis* Dps homolog; TfDPS, *Thermobifida fusca* Dps homolog; RmDPS, *Ralstonia metallidurans* Dps homolog. Alignment has been created with ClustalW2. Helical secondary structure elements are indicated at the top. The residues at the twofold and the ferritin-like threefold interfaces in EcDPS are highlighted in light grey and dark grey respectively. The residues mutated in this study are underlined.

the mutant Y16A formed a small amount (16%) of dimer along with 12-mer. Individual mutation of R83 or R133 resulted in 40% and 50% dimer formation respectively. Following this trend, double mutation of both these residues destroyed the ability of the protein to assemble into 12-mer, cleanly forming 100% dimer. This is consistent with the TEM micrographs, which showed that R83A/R133A produced no observable nano-cages.

Temperature-dependent CD analysis—Secondary structure, thermal stability, and reversibility after melting

None of the interfacial residues affect the ability of DPS to fold into an α-helical protein as evidenced by prominent minima at 208 and 222 nm in the CD spectra of the proteins (Supporting Information Fig. S9), although all the mutants exhibited reduced secondary structure. The lone exception is DPS D78A,

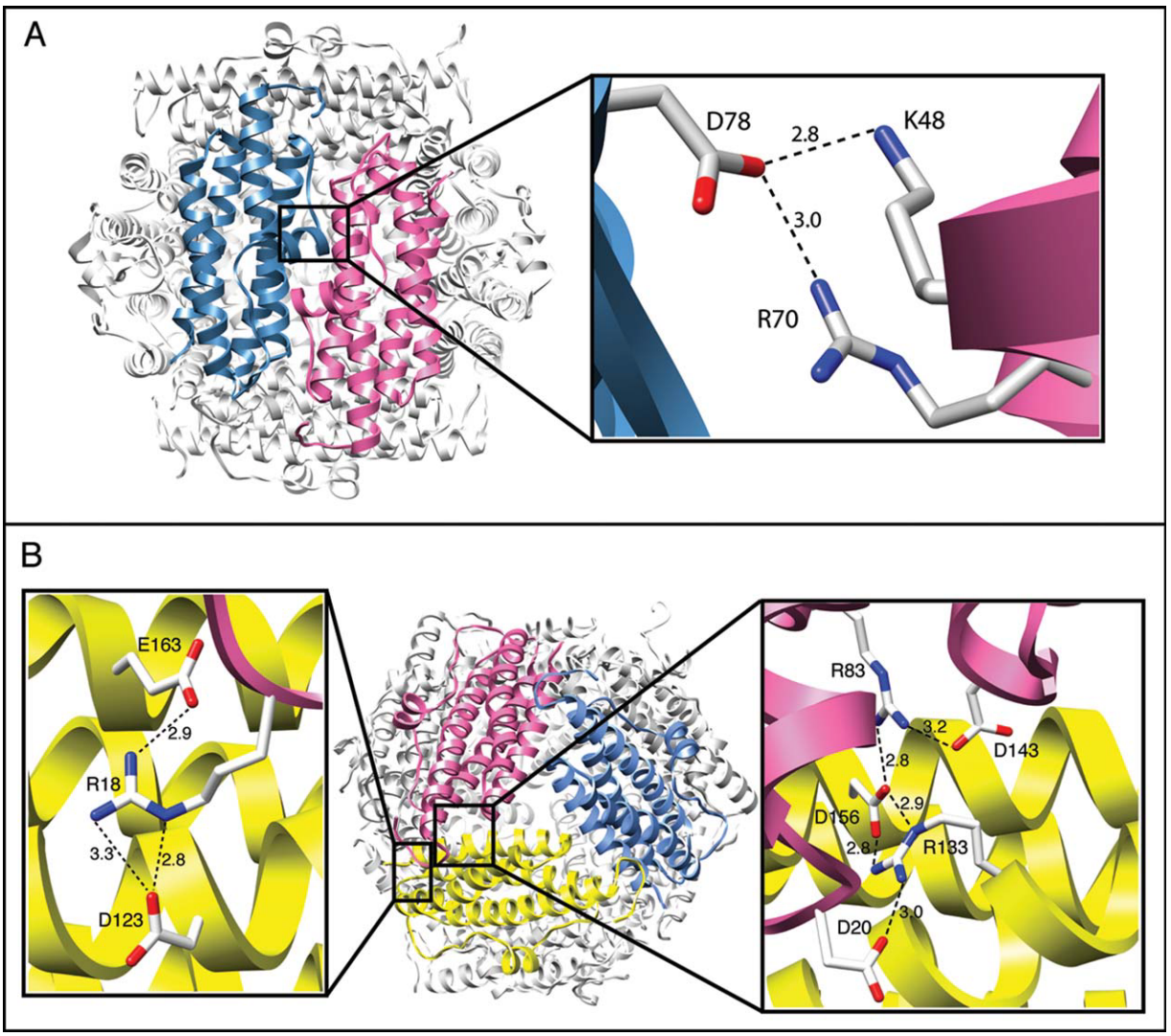

Figure 4. Hydrogen bonding networks at the DPS twofold and ferritin-like threefold symmetry interfaces. (A) Twofold symmetry interface (left) and expansion of the interaction between D78, K48, and R70 (right). (B) Ferritin-like threefold symmetry interface (middle) and expansion of the interaction between R83, R133, D156, D143, D20 (right) and between R18, E163 and D123 (left). The heavy atom distances between the interacting groups are indicated as dotted lines and the distances are given in Å.

which gives a nearly identical spectrum to DPS itself. The residue that causes the greatest reduction in structure upon mutation is W160. The double mutant, R83A/R133A, is less structured than its respective single mutants.

Increasing the temperature results in the melting of the secondary structure (Supporting Information Figs. S8 and S9). By monitoring the 222 nm band, it is evident that, for all the proteins, this unfolding is cooperative, and that these residues do not control the ability of DPS to form a tight, stable fold. Most of the mutants melt at a lower temperature than wild-type DPS, demonstrating that even single interfacial mutations can affect the protein thermal stability. The exception to this trend is D146A which has nearly identical stability as wild-type DPS. The residues that affect the stability the greatest upon single mutation to alanine are R83 and R133. Destruction of this hydrogen bond cluster by combining these two mutations predictably results in a protein, DPS R83A/R133A, with a melting point depressed by nearly 25°C.

Slowly reducing the temperature following thermal melting allows for the exploration of folding reversibility (Supporting Information Fig. S9) by comparing the structure before and after the melt. Although some visible precipitation for a few of the mutants was observed under these conditions, poor reversibility was also observed for the wild-type protein, suggesting that this is a property of DPS itself and not due to mutagenesis. Although no clear trends are evident, thermal stability does not seem to follow that of reversibility which is consistent with other work we have done in these systems.[18,19] Interestingly, the double mutant R83A/R133A, which was the least stable, is among the most reversible

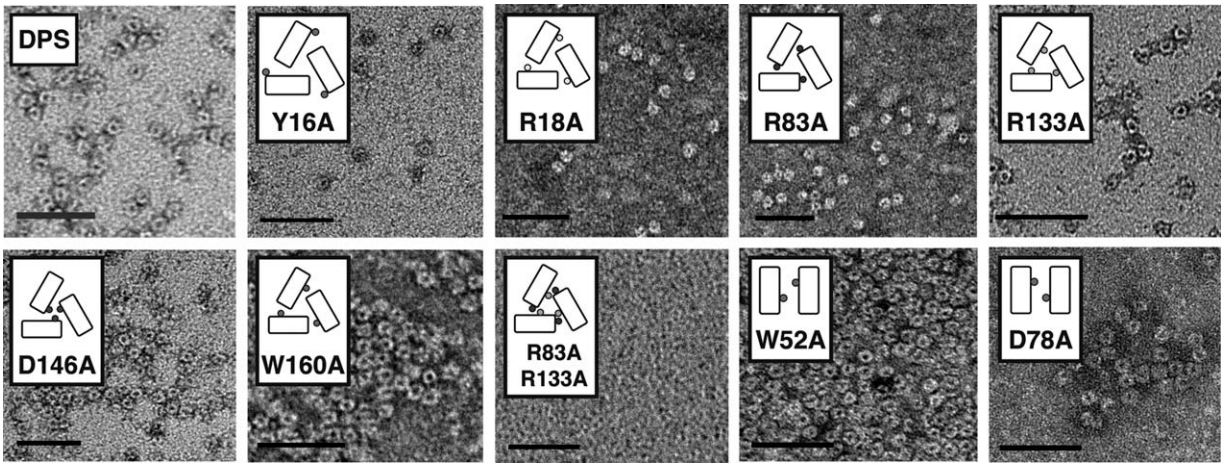

Figure 5. All single mutants can form nano-cages in TEM conditions. Negatively stained TEM micrographs indicate that all of the DPS-derived single mutants can form nano-cages. Scale bars indicate 50 nm. Schematics follow the convention in Figure 2.

which is possibly due to the fact that it only forms dimer in solution. As we have reported that BFR alanine-shaved mutants were more reversible than the DPS series, the fact that the thermal stability of BFR was more sensitive to mutation than was DPS, suggests that that competing thermodynamic versus kinetic control exists in the unfolding of the two proteins, or simply that an aggregation pathway is more accessible to DPS in general.

Discussion

The ferritin-like DNA-binding protein from starved cells (DPS), from *E. coli* was used in this study with the goal of building upon the established fundamentals of protein-protein interactions and self-assembly. In analogy to our work with *E. coli* bacterioferritin (BFR), DPS was subjected to a strategy where amino acids at protein-protein interfaces were mutated to identify residues that control assembly and stability.[19] As opposed to traditional "alanine shaving" studies where the energetic role of each residue is determined relative to the wild-type through the measurement of the equilibrium between the oligomerized state and disassociated state, our strategy, due to the complexities associated with highly oligomeric structures and mathematical challenges in measuring their equilibrium, focused on measuring the energetic effect of mutating a residue to alanine on the equilibrium between the folded, oligomeric state and the unfolded, disassociated state through denaturation.[12,27]

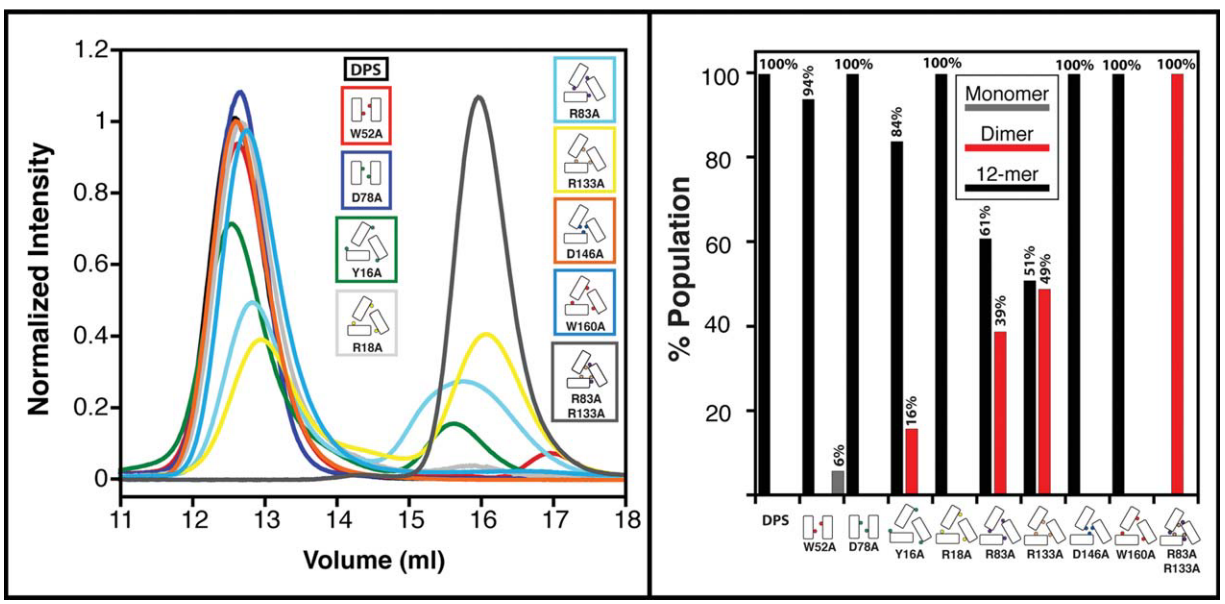

Figure 6. Two residues control the assembly from dimer to 12-mer. (Left) SEC chromatograms of the mutants. (Right) Quantitation of the populations determined from the SEC chromatograms with respect to oligomerization state. Schematics follow the convention in Figure 2.

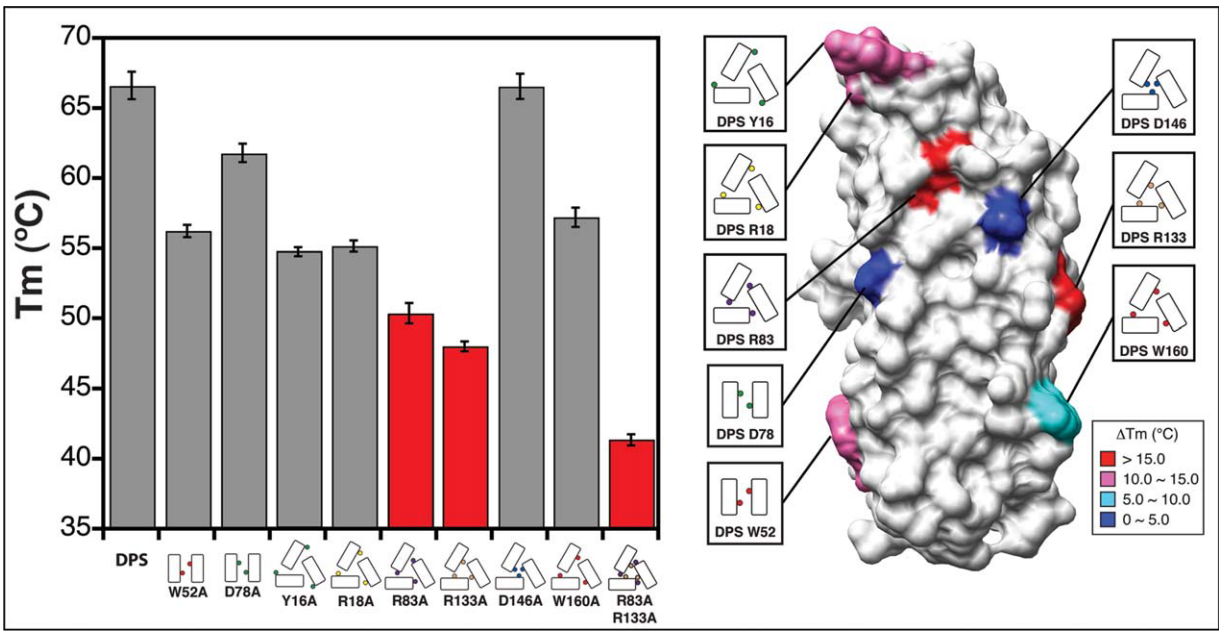

Figure 7. The identification of thermally significant interfacial residues. (Left) Quantified transition melting temperatures from the data presented in Supporting Information Figures S8 and S9. Schematics follow the convention defined in Figure 2. Error bars represent the standard deviation of three replicates. (Right) Residular thermal transition temperatures mapped onto a DPS monomer. (PDB ID: 1dps).

All nine of the mutants formed cooperatively folded α-helical structures (Supporting Information Fig. S9) and all the mutants, except the double mutant R83A/R133A, possessed the ability to form nano-cages as evidenced by SEC (Fig. 6) and TEM (Fig. 5). All DPS mutants melted at a lower temperature than did wild-type DPS (Fig. 7), suggesting that even single point mutations can affect protein thermal stability if they are at appropriate positions. Taken together, these data confirm that many of these residues are indeed hot spots and that hot spots can be rationally identified in some systems. Interestingly, residue D146, which is well conserved in the Dps family (Fig. 3) and was reported to be involved in iron uptake, has little effect on the protein stability and assembly of cage structure.

The most striking results involve R83 and R133. These residues, which are involved in an extended hydrogen bond network (Fig. 4) at the ferritin-like threefold symmetry axis and were, of the residues chosen for mutation, predicted to be the most energetically significant by virtual alanine scanning (Supporting Information Figs. S10 and S11). Moreover, arginine and lysine are found in similar positions in DPS from a diverse array of species (Fig. 3). The melting temperature (Tm) of mutants which shave the side chains of these residues individually were the lowest among the point mutants, and complete disruption of the hydrogen bond network through double mutation resulted in the least stable protein emphasizing the importance of these residues. The key role of these residues is further enforced by the fact that individual mutation of R83 and R133 to alanine results in proteins that form a mixture of 12-mer and a substantial amount of dimer (39% and 49%, respectively). Consistent with the thermal profile, combining these mutations results in a protein that only forms dimer. TEM also confirms that mutating these residues results in protein cage disassembly.

Previous work with Dps homologs has revealed that it is possible to alter their oligomerization state with some proteins in specific conditions.[28,29] For example *Deinococcus radiodurans* Dps-1 was reported to switch from a 12-mer to a dimer upon buffer exchange from high to low salt[30] and the *Listeria innocua* DPS 12-mer can be made to dissociate to a dimer by lowering the pH below 2.0.[31] Moreover, Dps from *Mycobacterium smegmatis* dissociates into lower order oligomers at low temperature (4°C).[32,33] These examples all involve changing solution conditions, and while they may be providing relevant information that can be extrapolated, ways to alter the oligomerization state in standard conditions with minimal perturbation are necessary for delivery and materials applications and for example, as controls to understand the role of oligomerization in DNA binding. The few mutants that have been discovered to alter the Dps oligomerization state involved deletions of relatively large subdomains that have been implicated in other roles such as making interactions with DNA or in iron transport.[34] Therefore, the discovery of a simple double mutant that cleanly alters the oligomerization state not only provides insight into

fundamentals of this system, it could also provide direction to the development of unique applications and better tools to explore the role oligomerization plays in DNA binding,[30] the design of a switchable protein container, as a control for high throughput assays for screening protein libraries for enhance oligomerization or as a first step to design a protein that can form alternative oligomerization states.

The straightforward rationality of this system is further emphasized through recalling that these two residues are located at the ferritin-like threefold symmetry axis and hence a trimer interface. It is reasonable that the destabilization of this threefold symmetry would result in a protein with an intact twofold interface which would still allow the formation of an antiparallel dimer that is shared across the ferritin cages, including the maxi- and mini-ferritins. Some assembly mechanisms have invoked similar dimer intermediates although others have proposed trimers and dimers which are not necessarily related to the symmetry of the fully assembled cage.[35] For example, Gupta *et al.* found that *M. smegmatis* Dps supported a trimer-dependent assembly mechanism with two stable oligomeric forms of trimer and dodecamer.[33] However, the lack of observed trimers does not necessarily rule out a mechanism involving trimer intermediates that are short lived on the experimental time frame.[36] Moreover, *E. coli* Dps may have an oligomerization mechanism unique from that of other proteins in the family. Additionally, the enhanced reversibility of the mutants that only form dimers could be a consequence of a simpler assembly mechanism; the fewer the possible intermediates, the fewer chances there are for misassembly resulting in aggregation. An alternative, and it should be noted, equally speculative, explanation would involve pointing out that through mutation, we may not only be altering the ground state energetics but the energies of transition states as well, which would surely affect the metastability of the oligomerized state opening up irreversibility which manifests as aggregation.[37] Our mutants may be useful tools to understand these mechanisms and states. In addition, as our stated long-term goal is to convert a mini-ferritin-forming monomer into one that assembles into a maxi-ferritin, and vice versa, this research where we have learned how to logically disassemble a mini-ferritin into an intermediate that may be common to both types of cages would be a reasonable initial step.

It is useful to compare the results of this study with those using the maxi-ferritin BFR. In that previous research, we discovered four residues that completely obliterate cage formation when mutated to alanine.[19] Surprisingly, one of these is located at the twofold axis of symmetry suggesting that there either is a global conformational change or that an oligomerization nonproductive dimer is possible. In addition, we also discovered two residues that increase the overall stability of the protein when mutated. This result is remarkable not only in that overall thermal and chemical stability was enhanced, but that both of these mutations only form dimer. In addition, in a recent study to examine the importance of water pockets at a maxi-ferritin twofold symmetry axes and the possibility of exploiting them to generate proteins with enhance stability, we proposed the presence of a nonproductive dimer to explain the discovery of other mutants that were more thermally stable but only formed dimer. We imagine that these dimers would not be unlike an architectural keystone exposing faces of improper relative angles to span an arch of a desired diameter. We referred to this as the "Arch and Keystone" hypothesis, the possibility of which we are currently exploring.[38] These complexities contrasted with the relatively very rational and straightforward DPS, further emphasizing the structural energetic distinctness of these mini- and maxi-ferritins. Furthermore, fundamental studies of how protein-protein interactions control the stability and oligomerization of cage proteins could aid in the development of future applications, provide controls for further studies, and direct investigations into using these proteins as building blocks in the design and discovery of novel oligomerized architectures.

Materials and Methods

Virtual alanine scanning

Web tools developed by the Baker lab were used for the virtual detection of amino acid residues that make significant contributions to the energetics of the protein-protein interfaces.[24] The input for this analysis was modified from the crystal structure coordinates for DPS (PDB ID: 1dps). Two monomers at the twofold axis and three monomers around two, nonequivalent threefold axes were used. The output of the computational analysis predicted a "hot spot" if the $\Delta\Delta G$ for mutagenesis to alanine was greater than 1 kcal/mol. The results are displayed in tabular form in Supporting Information Figures S10–S12.

Cloning, protein expression, and purification

All the genes were cloned into pET-32 Ek/LIC vector (Novagen). The constructs were transformed into *E. coli* BL21 (DE3) (Novagen) electrocompetent cells. Proteins were purified by affinity chromatography, followed by gel filtration. Detailed procedures are described in the Supporting Information.

Transmission electron microscopy (TEM)

Purified protein (20 $\mu g\ mL^{-1}$) was stained using uranyl acetate (1% w/v). TEM data was obtained using

a JOEL JEM-1400 microscope operating at 120 keV. Captured TEM micrographs were analyzed using ImageJ (NIH) to measure the longest diameter of the protein cages. For each protein, 100 particles were measured except for DPS Y16A where only 50 particles were measured (Fig. 5 and Supporting Information Fig. S7).

Size exclusion chromatography (SEC)

Size exclusion chromatography experiments were performed on an ÄKTAFPLC™ (GE Healthcare) system equipped with a UV detector ($\lambda = 280$ nm) using a Superdex 200 10/300 GL gel filtration column pre-equilibrated with running buffer (50 m*M* NaH_2PO_4, 150 m*M* NaCl, pH 7.0). The SEC experiments were all conducted at 4°C with a flow rate 0.5 mL/min. The column was previously calibrated using six well-characterized proteins as standards (GE Biosystems Calibration Kit)[18] (Supporting Information Figs. S5 and S6). Oligomerization state was determined from the calculated molecular weight and the predicted monomer molecular weight (Fig. 6).

Temperature-dependent CD analysis

CD spectra were monitored and collected on a Jasco J-810 spectropolarimeter equipped with a Peltier temperature controller in the far-UV range (200–250 nm) using a 1 mm quartz cell. Protein solution concentration was determined (BCA Protein Assay Kit, Novagen), and the solution was diluted (100 μg mL^{-1}) with phosphate buffer (50 m*M* NaH_2PO_4, pH 7.2). Ellipticity was measured at 222 nm and the temperature was increased from 20 to 90°C in 5°C steps. Samples were allowed to equilibrate for 8 min at each temperature. After melting, the protein solutions were cooled slowly to 20°C over 10 min, and the resulting spectra were compared with those obtained before unfolding. At least three replicates were performed (Fig. 7 and Supporting Information Figs. S8 and S9).

Acknowledgment

The authors thank Maziar Ardejani for helpful discussions.

References

1. Dosztanyi Z, Chen J, Dunker AK, Simon I, Tompa P (2006) Disorder and sequence repeats in hub proteins and their implications for network evolution. J Proteome Res 5:2985–2995.
2. Orner BP, Ernst JT, Hamilton AD (2001) Toward proteomimetics: terphenyl derivatives as structural and functional mimics of extended regions of an alpha-helix. J Am Chem Soc 123:5382–5383.
3. Fan RL, Chew SW, Cheong VV, Orner BP (2010) Fabrication of gold nanoparticles inside unmodified horse spleen apoferritin. Small 6:1483–1487.
4. Klem MT, Willits D, Solis DJ, Belcher AM, Young M, Douglas T (2005) Bio-inspired synthesis of protein-encapsulated CoPt nanoparticles. Adv Funct Mater 15: 1489–1494.
5. Meldrum FC, Wade VJ, Nimmo DL, Heywood BR, Mann S (1991) Synthesis of inorganic nanophase materials in supramolecular protein cages. Nature 349: 684–687.
6. Uchida M, Klem MT, Allen M, Suci P, Flenniken M, Gillitzer E, Varpness Z, Liepold LO, Young M, Douglas T (2007) Biological containers: protein cages as multifunctional nanoplatforms. Adv Mater 19:1025–1042.
7. Uchida M, Flenniken ML, Allen M, Willits DA, Crowley BE, Brumfield S, Willis AF, Jackiw L, Jutila M, Young MJ, Douglas T (2006) Targeting of cancer cells with ferrimagnetic ferritin cage nanoparticles. J Am Chem Soc 128:16626–16633.
8. Worsdorfer B, Woycechowsky KJ, Hilvert D (2011) Directed evolution of a protein container. Science 331: 589–592.
9. Orner BP, Liu L, Murphy RM, Kiessling LL (2006) Phage display affords peptides that modulate beta-amyloid aggregation. J Am Chem Soc 128:11882–11889.
10. Ren Y, Wong SM, Lim LY (2007) Folic acid-conjugated protein cages of a plant virus: a novel delivery platform for doxorubicin. Bioconjugate Chem 18:836–843.
11. Weiss GA, Watanabe CK, Zhong A, Goddard A, Sidhu SS (2000) Rapid mapping of protein functional epitopes by combinatorial alanine scanning. Proc Natl Acad Sci USA 97:8950–8954.
12. Cunningham BC, Wells JA (1989) High-resolution epitope mapping of hgh-receptor interactions by alanine-scanning mutagenesis. Science 244:1081–1085.
13. Jin L, Wells JA (1994) Dissecting the energetics of an antibody-antigen interface by alanine shaving and molecular grafting. Protein Sci 3:2351–2357.
14. Grant RA, Filman DJ, Finkel SE, Kolter R, Hogle JM (1998) The crystal structure of Dps, a ferritin homolog that binds and protects DNA. Nat Struct Biol 5: 294–303.
15. Carrondo MA (2003) Ferritins, iron uptake and storage from the bacterioferritin viewpoint. EMBO J 22: 1959–1968.
16. Liu XF, Theil EC (2005) Ferritins: dynamic management of biological iron and oxygen chemistry. Accounts Chem Res 38:167–175.
17. Theil EC (2011) Ferritin protein nanocages use ion channels, catalytic sites, and nucleation channels to manage iron/oxygen chemistry. Curr Opin Chem Biol 15:304–311.
18. Fan R, Boyle AL, Cheong VV, Ng SL, Orner BP (2009) A helix swapping study of two protein cages. Biochemistry 48:5623–5630.
19. Zhang Y, Raudah S, Teo H, Teo GWS, Fan RL, Sun XM, Orner BP (2010) Alanine-shaving mutagenesis to determine key interfacial residues governing the assembly of a nano-cage maxi-ferritin. J Biol Chem 285: 12078–12086.
20. Lawson DM, Treffry A, Artymiuk PJ, Harrison PM, Yewdall SJ, Luzzago A, Cesareni G, Levi S, Arosio P (1989) Identification of the ferroxidase centre in ferritin. Febs Lett 254:207–210.
21. Bellapadrona G, Stefanini S, Zamparelli C, Theil EC, Chiancone E (2009) Iron translocation into and out of *Listeria innocua* Dps and size distribution of the protein-enclosed nanomineral are modulated by the electrostatic gradient at the 3-fold "ferritin-like" pores. J Biol Chem 284:19101–19109.
22. Krissinel E, Henrick K (2007) Inference of macromolecular assemblies from crystalline state. J Mol Biol 372: 774–797.

23. Jencks WP (1981) On the attribution and additivity of binding-energies. Proc Natl Acad Sci USA 78:4046–4050.
24. Kortemme T, Kim DE, Baker D (2004) Computational alanine scanning of protein-protein interfaces. Sci STKE 2004:pl2.
25. Chiancone E, Ceci P (2010) The multifaceted capacity of Dps proteins to combat bacterial stress conditions: detoxification of iron and hydrogen peroxide and DNA binding. Biochim Biophys Acta 1800:798–805.
26. Swift J, Wehbi WA, Kelly BD, Stowell XF, Saven JG, Dmochowski IJ (2006) Design of functional ferritin-like proteins with hydrophobic cavities. J Am Chem Soc 128:6611–6619.
27. Jaenicke R, Rudolph R (1986) Refolding and association of oligomeric proteins. Methods Enzymol 131: 218–250.
28. Chowdhury RP, Vijayabaskar MS, Vishveshwara S, Chatterji D (2008) Molecular mechanism of in vitro oligomerization of Dps from *Mycobacterium smegmatis*: mutations of the residues identified by interface cluster analysis. Biochemistry 47:11110–11117.
29. Chowdhury RP, Saraswathi R, Chatterji D (2010) Mycobacterial stress regulation: the Dps twin sister defense mechanism and structure-function relationship. IUBMB Life 62:67–77.
30. Grove A, Wilkinson SP (2005) Differential DNA binding and protection by dimeric and dodecameric forms of the ferritin homolog Dps from *Deinococcus radiodurans*. J Mol Biol 347:495–508.
31. Chiaraluce R, Consalvi V, Cavallo S, Ilari A, Stefanini S, Chiancone E (2000) The unusual dodecameric ferritin from *Listeria innocua* dissociates below pH 2.0. Eur J Biochem 267:5733–5741.
32. Ceci P, Ilari A, Falvo E, Giangiacomo L, Chiancone E (2005) Reassessment of protein stability, DNA binding, and protection of *Mycobacterium smegmatis* Dps. J Biol Chem 280:34776–34785.
33. Gupta S, Chatterji D (2003) Bimodal protection of DNA by *Mycobacterium smegmatis* DNA-binding protein from stationary phase cells. J Biol Chem 278: 5235–5241.
34. Roy S, Saraswathi R, Gupta S, Sekar K, Chatterji D, Vijayan M (2007) Role of N and C-terminal tails in DNA binding and assembly in Dps: structural studies of *Mycobacterium smegmatis* Dps deletion mutants. J Mol Biol 370:752–767.
35. Roy S, Gupta S, Das S, Sekar K, Chatterji D, Vijayan M (2004) X-ray analysis of *Mycobacterium smegmatis* Dps and a comparative study involving other Dps and Dps-like molecules. J Mol Bio 339:1103–1113.
36. Zhang Y, Orner BP (2011) Self-Assembly in the ferritin nano-cage protein superfamily. Int J Mol Sci 12: 5406–5421.
37. Baldwin AJ, Knowles TP, Tartaglia GG, Fitzpatrick AW, Devlin GL, Shammas SL, Waudby CA, Mossuto MF, Meehan S, Gras SL, Christodoulou J, Anthony-Cahill SJ, Barker PD, Vendruscolo M, Dobson CM (2011) Metastability of native proteins and the phenomenon of amyloid formation. J Am Chem Soc 133: 14160–14163.
38. Ardejani MS, Li NX, Orner BP (2011) Stabilization of a protein nanocage through the plugging of a protein-protein interfacial water pocket. Biochemistry 50: 4029–4037.